

Supplementary information: Nanomechanical mapping of single collagen fibrils under tension

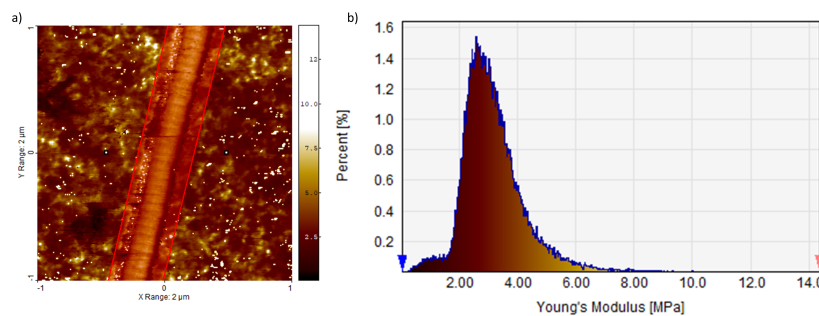
Chris J. Peacock, Laurent Kreplak

1 Substrate stiffening as a response to applied strain

The PDMS modulus was measured as a function of applied strain, for the purposes of comparing to measurements made in a previous study¹. What follows is a brief description of the method used to extract PDMS modulus, as well as a summary of modulus values obtained from all images captured in this study.

1.1 PDMS indentation modulus extraction

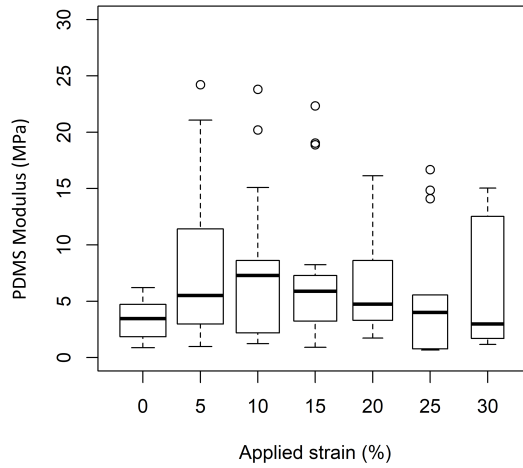
The PDMS modulus values were extracted from the same nanomechanical maps that the fibril modulus profiles were obtained from. A region of exclusion was drawn around the fibril in each image (figure S1a), and a histogram was constructed from all the non-excluded pixel values (figure S1b). A moving 10-bin average was applied to the histogram data, and the position of the largest peak in the regional average curve was recorded as the modulus of the PDMS in the image.



S 1: a) An example of a nanomechanical map from which a distribution of PDMS modulus values are obtained. A 200-300nm wide region around the fibril is excluded (in red) from the b) distribution of substrate modulus value.

1.2 Results and Discussion

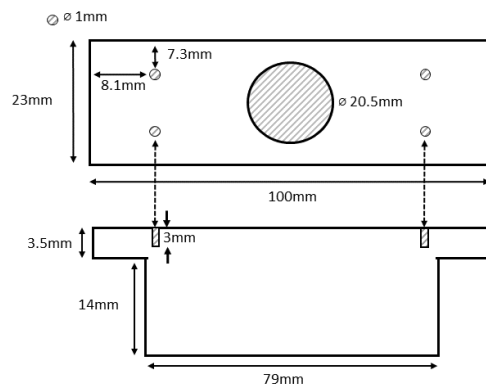
Figure S2 presents the indentation modulus of all 8 PDMS substrates as a function of the strain applied by the motors. Before strain was applied to PDMS, an average modulus of 3.3 ± 1.6 MPa ($n=8$) was obtained at a peak force frequency of 1kHz, which is in excellent agreement with measurements made by Nair et al¹. Subsequent increments of strain increased the range of modulus values measured, however the change in modulus was not monotonic with applied strain and furthermore was not consistent between PDMS strips. The median PDMS modulus value was found to vary little from the median of measurement made on unstrained PDMS (from 4MPa at the unstrained state to a maximum median of 7MPa at 10% applied strain), however the range of measurements increased dramatically. This increase in modulus range is likely due to the inhomogeneous straining of the PDMS, in part caused by the effect that the adsorbed fibril has on the strain field within $1\mu\text{m}$ of where the PDMS modulus measurements are made. As an example of this inhomogeneous straining, in figure S8 the topography of the PDMS can be seen to become rougher as what appears to be local tears form in the PDMS surface with applied strain.



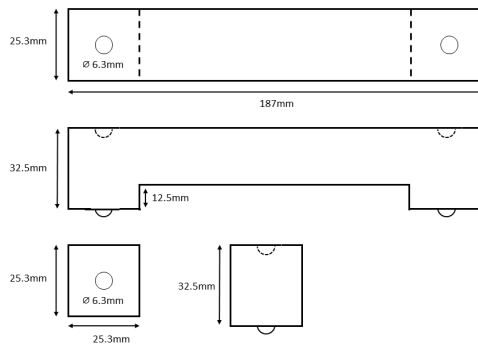
S 2: PDMS modulus versus applied strain. The thick black bar represents the median value, the box represents the first quartile of the set, the dotted bars represent the range of data.

2 Motorized stage extension components, with description

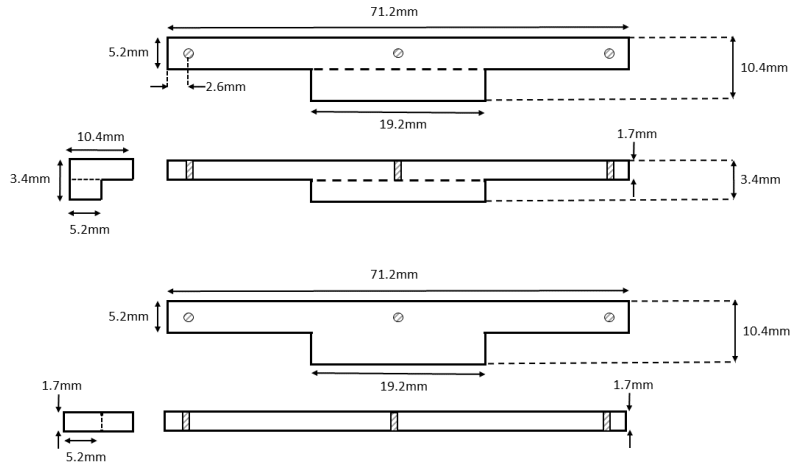
Here is a set of illustrated diagrams of the components of the motorized stage (with dimensions) used to stretch the PDMS substrate. Excluded here is a schematic of the MM-1M linear stage used to strain the sample; information on this component can be found on the National Aperture website (National Aperture)



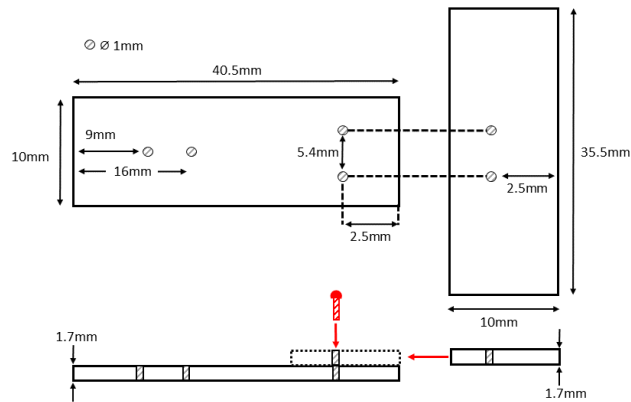
S 3: *The stage extension on which two motors were attached for sample straining. The central hole drilled into the piece allows for a long working-distance microscope objective to observe the strain substrate from the bottom-up.*



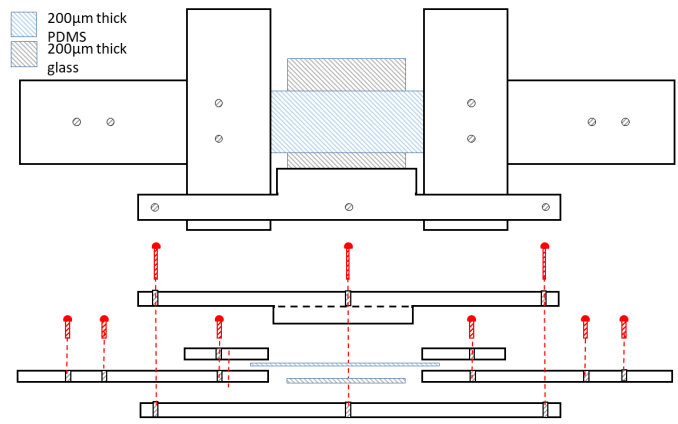
S 4: *A pair of stilts, used to extend the AFM scanning head to allow for scanning of the sample while clamped into the motorized stage extension.*



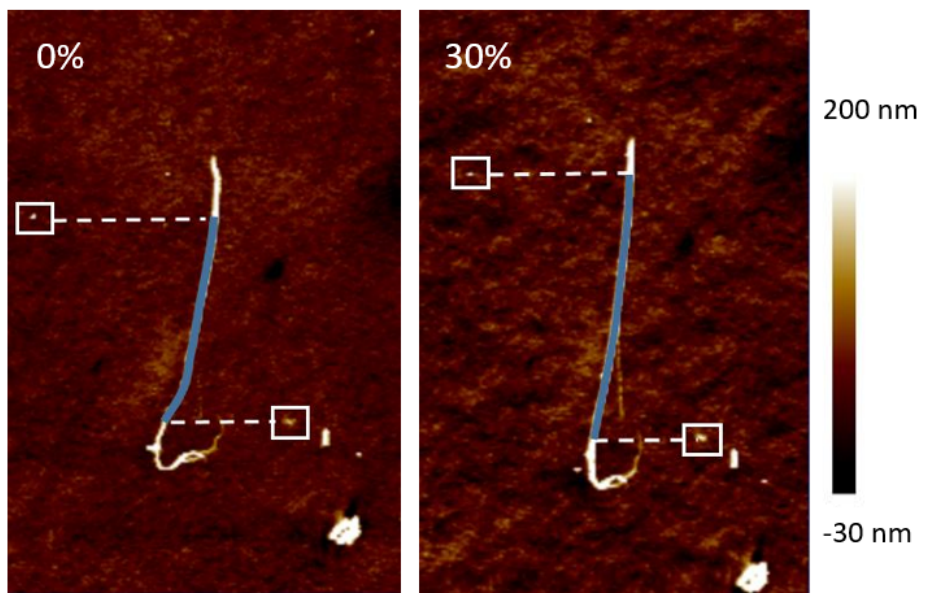
S 5: A cross-bar clamp used to support a glass microscope slide placed underneath the strained substrate during nanomechanical mapping. Without the microscope slide in place beneath the sample, the AFM cannot scan the sample in contact mode due to induced oscillations of the free-standing PDMS membrane.



S 6: A sample clamp installed on each of the two motors, used to hold each end of the PDMS membrane. The cross-bar clamp used to hold the glass slide beneath the sample is fixed to the wide section of this clamp.



S 7: *The sample clamps and crossbar clamp assembled in the configuration used during sample imaging. Below is a side-view of the assembled piece.*



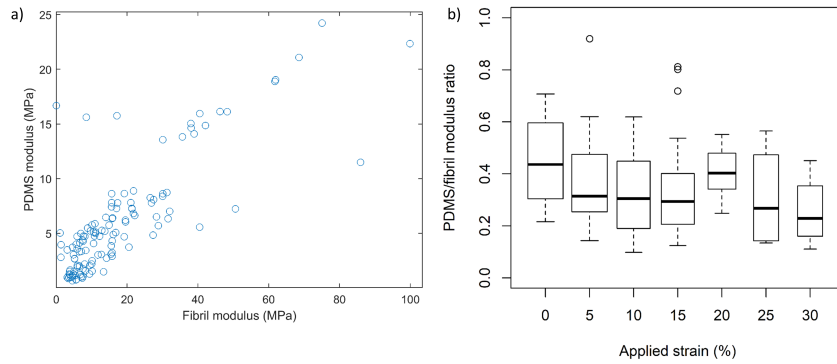
S 8: Fiducial strain is measured as the change in length of a section of the fibril (outlined in blue) measured between two fiducial markers (boxed in white for each image). The 0 and 30% labels in the top left corners refer to the strain applied to the substrate.

3 The substrate bottom effect on measured fibril indentation modulus

Bueckle’s rule applies to indentations made on materials (more accurately films) lying on a substrate, and states that bottom effects associated with indenting the film start to become relevant after indenting the film by 10-15% of its thickness². This rule assumes that the contrast in film-substrate stiffness is infinitely large. However, in the case of indenting collagen fibrils lying on PDMS, the ratio of indentation modulus between the PDMS and the fibril is close to unity (see figure S9a,b). In two separate studies, Antunes, Argatov and coworkers investigated theoretically the effect that indentation depth has on the measured indentation modulus of a film lying on a substrate, where the film and the substrate have an arbitrary modulus mismatch^{3,4}. The coefficient associated with indentations made with an axisymmetric indenter incorporates the modulus and Poisson’s ratio for each of the two materials in the system and is dependent on the contact radius of the indenter with the film, rather than the indentation depth.

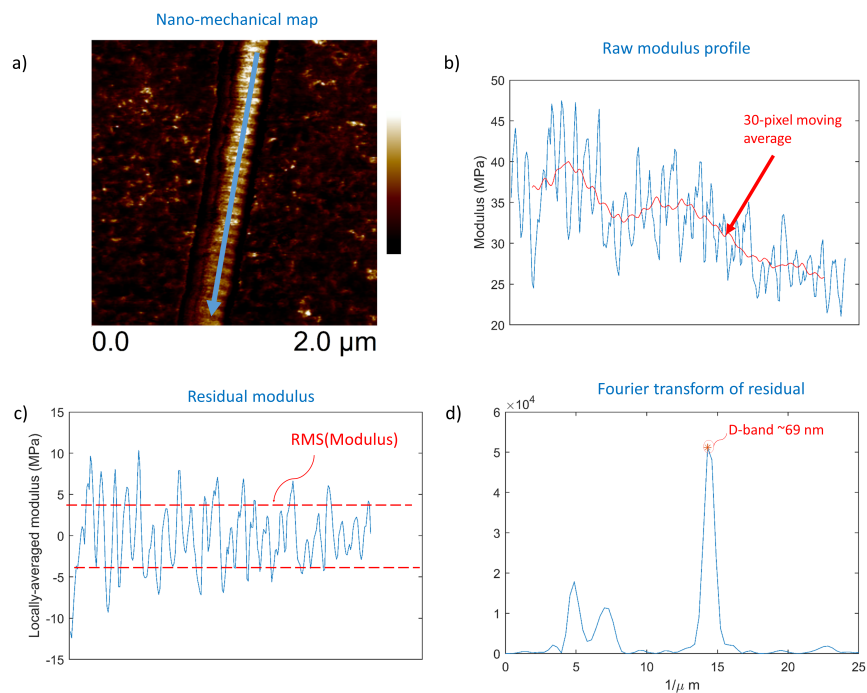
$$k = \frac{\eta}{1 + (\eta - 1)e^{-\alpha \frac{\eta}{(\eta-1)} \frac{a}{t}}} \quad (1)$$

In equation 1, k is the coefficient that is multiplied to the measured indentation modulus to correct for the bottom effect. The quantity $\eta = \frac{E_s^*}{E_f^*}$ is the ratio of the substrate and film modulus where E_f^* and E_s^* are the elastic moduli of the film and the substrate corrected by the Poisson’s ratio of each material respectively (ex: $E_s^* = \frac{E_s}{1-\nu_s^2}$). $\frac{a}{t}$ is the ratio of the indenter radius to the thickness of the film, and α_0 is a constant associated with the boundary conditions between the substrate and the film. By assuming that the Poisson’s ratios of the PDMS and of the Fibril are similar (0.5) and calculating the equivalent hemispherical contact radius of a cone with a half-angle of 18° indenting approximately 15% of the total fibrillary height, the coefficient k associated with the bottom-effect was found to be on the order 1.03-1.04. Ignoring this coefficient represent a 3-4% underestimate of the film modulus that is negligible compared to the intrinsic variations along individual fibrils (see figure S10b)). In addition, as the PDMS substrate was stretched, the magnitude of the modulus mismatch did not change significantly which means that the underestimate remained constant throughout the experiment (figure S9b).

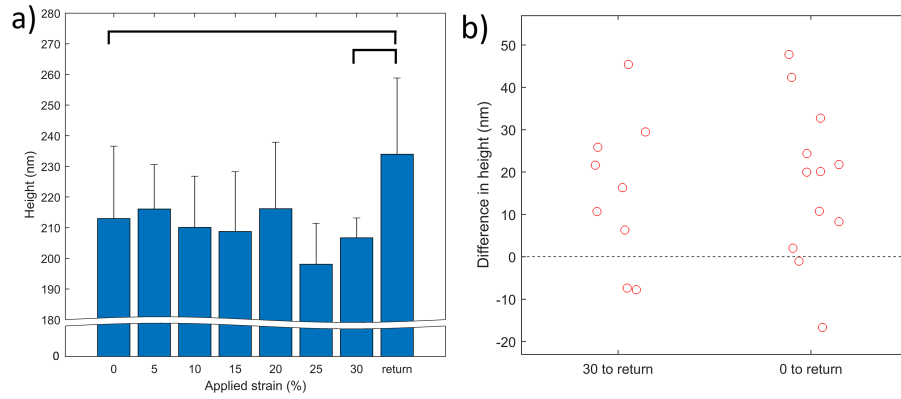


S 9: a) the modulus values measured on the PDMS are plotted versus the fibril modulus values from their respective nanomechanical maps. b) The PDMS-fibril modulus ratio is plotted as a function of applied strain. The thick black bar represents the median value, the box represents the first quartile of the set, the dotted bars represent the range of data. The median of the distribution of PDMS/fibril modulus ratios can be seen to decrease as a function of applied strain, which demonstrates that the two materials are mechanically distinct in how they respond to extension.

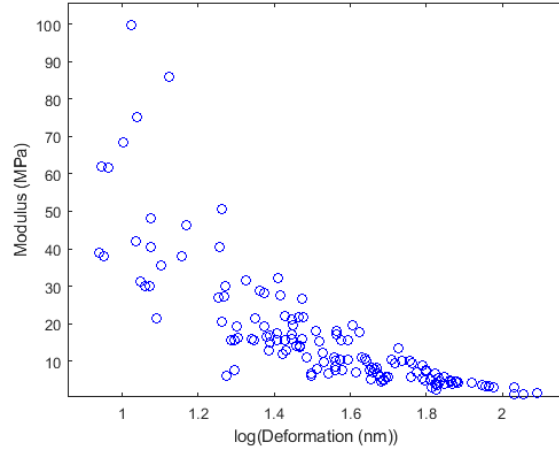
4 Supplementary Figures



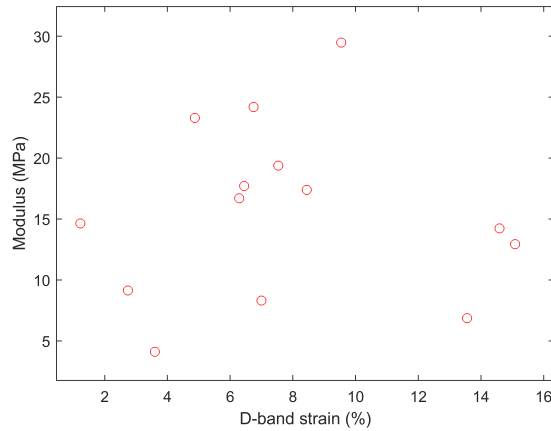
S 10: Description of D-band extraction procedure. a) A profile is drawn along the apex of the fibril in a nanomechanical map, b) a 30-pixel running average is calculated from the modulus profile and is subtracted from the profile to obtain a c) residual modulus signal. The root mean squared variation in this residual is recorded and used in calculating the gap-overlap modulus ratio. d) The frequency value corresponding to the peak in the Fourier transform of this residual modulus signal (between 10 and $20 \mu\text{m}^{-1}$) is recorded as the average D-band frequency of the fibril in the image.



S 11: a) Height as a function of applied strain, averaged over all regions measured. Brackets indicate significant change in height within the same region when comparing 0% with the return (paired Student's t -test, $p=3.30\times 10^{-3}$) and 30% strain with the return (paired Student's t -test, $p=4.00\times 10^{-3}$). b) Average height difference measured for each region when comparing 0% and 30% strain with the return, only significant differences are included (paired Student's t -test, $p\leq 0.05$). Swelling occurs upon return in at least 80% of the measured regions in both cases.



S 12: Indentation modulus plotted versus the logarithm of deformation. Note that at low deformation, the indentation modulus increases dramatically. This represents the low point density in the portion of the force curve to which the Sneddon model of indentation is fit, at low deformability.



S 13: Indentation modulus plotted versus D-band strain. Each red datapoint represents the 3-region average values of modulus and D-band strain. Interestingly, there does not seem to be a relationship between average indentation modulus and D-band strain.

5 High-resolution nanomechanical mapping

In an effort to strengthen the claim that the gap and overlap regions experience different amounts of strain when the fibril is held in tension, a series of high-resolution (2nm/pixel) nanomechanical maps were captured on a collagen fibril at several increments of applied strain.

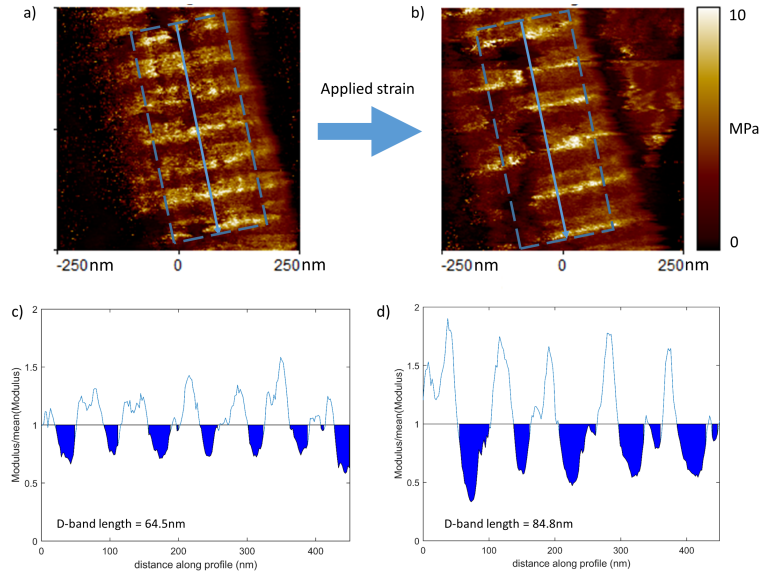
5.1 Materials and Methods

Following the sample preparation procedure outlined in the materials and methods section of the report collagen fibrils were dissected from a common digital extensor tendon, and were adsorbed to a PDMS film before being dried overnight. Note that the common digital extensor tendon used in the preparation of this sample was a separate specimen from the one used in the report, however the tissue was sourced from the same local slaughterhouse (Oulton farm, Nova Scotia, Canada) as before. The incremental straining experiment was repeated using the same protocol used in the materials and methods section of the report, however the resolution of the nanomechanical maps was increased to 2nm/pixel, by capturing $500\text{nm} \times 500\text{nm}$ images at 256 pixels/side. In addition, for the purposes of reducing the pressure applied by the tip to the sample when scanning at such high resolution, the peak force setpoint was reduced to 1nN, but otherwise all other parameters of the scan were kept to values outlined in the manuscript (a tip velocity of 1.2mm/s, a peak force frequency of 1kHz, a peak force amplitude of 300nm, and a scan rate of 0.5Hz).

5.2 Results and Discussion

Four high-resolution nanomechanical maps were acquired at 0, 5, 10 and 15% substrate strain. As mentioned in section 3.3.2, the D-band strain did not follow the substrate strain. So for our qualitative analysis we focused on the 0% and 10% substrate strain (figure S14a,b), as the latter nanomechanical map exhibited the largest D-band strain, 31%, compared to the two others.

The finer features in the overlap region were noticed to evolve in character as a function of strain (figure S14a,b; there is an increased contrast in stiffness between the two thin 'bands' making up the overlap). Deciding what features of the D-band stiffness striation constituted the start and end of the overlap region therefore became more subjective than quantitative. Rather than using arbitrary features along the length of the fibril to measure the gap and overlap lengths, a horizontal line was plotted through the modulus profile average, and the area between the regions above and below this line were compared before and after strain (figure S14c,d). From this treatment, the proportional difference between the size of the gap and overlap regions (ie., the relative areas above and below the average line) can be seen to change when the fibril is strained.



S 14: $500\text{nm} \times 500\text{nm}$ nanomechanical maps of a collagen fibril a) unstrained and b) in a strained state. c) and d) are 100-line averaged profiles drawn along the apex of the fibril in its unstrained and strained states, respectively. To demonstrate that the gap and overlap regions are changing in length a line was plotted through the average modulus value of each profile, and the area between the average-normalized profile and the straight line running through the average was filled.

References

- [1] S. S. Nair, C. Wang and K. J. Wynne, *Progress in Organic Coatings*, 2019, **126**, 119 – 128.
- [2] *The Science of hardness testing and its research applications.*, ed. J. H. Westbrook and H. Conrad, Metals Park, Ohio : American Society for Metals, 1973.
- [3] J. Antunes, J. Fernandes, N. Sakharova, M. Oliveira and L. Menezes, *International Journal of Solids and Structures*, 2007, **44**, 8313 – 8334.
- [4] F. J. S. Ivan I. Argatov, *International Journal of Engineering Science*, 2014, **81**, 33–40.